A Model for Drying of Viscoelastic Polymer Coatings

Richard A. Cairncross
Dept. of Chemical Engineering and Materials Science, University of Minnesota, Minneapolis, MN 55455

Christopher J. Durning
Dept. of Chemical Engineering, Materials Science, and Mining, Columbia University, New York, NY 10025

Drying of polymeric coatings often occurs under conditions where the relaxation time of polymer molecules is significant with respect to the processing time scales. The nonequilibrium thermodynamic theory of Durning and Tabor (1986) is applied to model 1-D drying of viscoelastic solutions with concentration-dependent physical properties. Transport of solvent to the surface of the coating occurs by viscoelastic diffusion down the gradient of a diffusion potential with a relaxing, nonequilibrium contribution. Galerkin's method with finite-element basis functions and a differential/algebraic equation system solver enable efficient solution of this stiff nonlinear model. Predictions show that elasticity enhances diffusion within the coating. At high Deborah numbers, however, a fall in the surface activity slows the rate of desorption. The coating thickness after a specified time under fixed total driving force is the smallest at intermediate Deborah numbers, showing that a small amount of viscoelasticity actually aids in drying. This can be interpreted as a skinning effect.

Introduction

The properties of coatings depend frequently upon the process by which the liquid precursor is dried or solidified after deposition. Skinning refers to the nonhomogeneous drying or solidification under large driving forces, where the top, drying surface of the coating and the deeper coating liquid have drastically different properties. This is a commonly reported phenomenon in the production of coated films, fibers, and particles from liquid solution or suspension. Several processes exist where skinning is a desirable phenomenon. Membrane production by phase inversion or phase separation relies upon skin formation to create a dense microstructure near the surface of the coating while the bulk of the coating has a looser, porous microstructure (Anderson and Ullman, 1973; Tsay and McHugh, 1990; Shojaie et al., 1992). Skinning is also desirable in some spray drying operations to produce hollow microspheres (Charlesworth and Marshall, 1960). Normally, however, skinning is not desired in coating processes, because it can lead to stress development, deformation or cracking of the surface of the coating, decreased drying rates, retention of bubbles within the coating, and nonuniform microstructure or chemical composition through the coating. An important objective of this article and companion studies (Cairncross et al., 1992, 1995a) is to develop computer-aided predictions of the conditions that cause skinning and thereby determine drying protocols under which skinning can be controlled or eliminated.

There are several physical interpretations of skinning in the coating literature including *figurative skinning*, in which steep concentration, and therefore physical property gradients arise near the surface of the coating; *literal skinning*, in which a distinct surface layer develops with elastic or solid-like properties, while the deeper material is still liquid (Cairncross, 1992, 1995a); and *trapping skinning*, in which by some mechanism, more severe drying conditions (such as higher airflow or lower external solvent pressures) cause more solvent to be trapped within the coating (Crank, 1950a; Powers and Collier, 1990). The experimental evidence for trapping skinning is not well documented, but it is commonly reported by practitioners in the field. Any of these three skinning phenomena may occur individually or in combination during a drying process.

Correspondence concerning this article should be addressed to R. A. Cairncross at his current address: Mechanical Engineering Dept., University of Delaware, Newark, DE 19716.

Figurative skinning occurs when appreciable internal resistance to mass transfer exists during drying and results in nonuniform properties. Literal skinning is caused by the emergence of elasticity due to curing or phase transformations within the coating; it is often accompanied by stress development within the skin which may lead to wrinkles, crazing, or cracking. Trapping skinning may be caused by a time lag in physical property changes after application of the driving force due to relaxation (in polymers), reaction, or phase transformation, and results in excessive solvent retention within the coating. Despite numerous reports by industrial practitioners, trapping skinning has not been considered experimentally or theoretically in fundamental studies. Crank (1950b, 1956) showed that Fickian diffusion cannot explain trapping skinning; so, other mechanisms such as polymer relaxation, phase transformation, and chemical reactions must be responsible for these observations. This article investigates whether viscoelasticity can explain trapping skinning during the drying of polymer solutions.

In the continuum limit, mutual diffusion in polymer-simple fluid mixtures does not, generally, obey Fick's laws. The nature of these deviations has been studied in model systems, both above and below the gas transition by sorption (Thomas and Windle, 1978; Hui et al., 1987; Lasky et al., 1988; Vrentas et al., 1986; Billovits and Durning, 1993, 1994) and light scattering (Nicolai et al., 1990a,b; Brown and Stepanek, 1993; Wang and Zhang, 1993; Sun and Wang, 1993). The deviations clearly arise from the effects of viscoelasticity and/or anelasticity on the interdiffusion. Roughly speaking, interdiffusion induces local, dilation-dominated deformation of the polymer component, which results in a relaxing or rate-dependent contribution to the local driving force for diffusion that we call the *nonequilibrium contribution to the diffusion potential.* It appears that the anelastic mechanisms affecting interdiffusion are closely related to, if not identical with, those detected mechanically in polymer-fluid mixtures (Nicolai et al., 1990a; Wang and Zhang, 1993; Billovits and Durning, 1994).

At present, there is no general agreement in the field as to exactly how viscoelasticity or anelasticity couple with diffusion. During the past decade, a number of first-principles treatments have been proposed (Neogi, 1983; Durning and Tabor, 1986; Carbonell and Sarti, 1990; Milner, 1991; Wang, 1991, 1992; Lustig et al., 1992; Govindjee and Simo, 1993; Jou et al., 1993; Beris and Edwards, 1994), but only a few (Durning and Tabor, 1986; Lustig et al., 1992; Wang, 1991, 1992) have been compared carefully with experiment (Billovits and Durning, 1994; Lustig, 1994; Brown and Stepanek, 1993; Wang and Zhang, 1993; Sun and Wang, 1993). For one-dimensional (1-D) sorption, the theories of Durning and Tabor (1986) and of Lustig et al. (1992) yield essentially the same mathematical model, which captures the essential features reported in sorption experiments (Billovits and Durning, 1993). Although more basic work is clearly needed to understand light scattering results, and to reconcile the various theories proposed, it appears that the common model derived from Durning and Tabor (1986) and Lustig et al. (1992) is at least qualitatively reliable, if not quantitatively accurate for 1-D sorption in concentrated polymer-simple fluid mixtures. Consequently, we utilize this model in a description of 1-D drying of a viscoelastic solution.

Theory

For 1-D sorption of a simple fluid into a polymer slab with viscoelastic properties, Durning et al. (1985, 1986) suggest that diffusion occurs down a gradient of a potential, with a nonequilibrium, relaxing component. In "polymer material" coordinates (Billovits and Durning, 1989), the constitutive equation for the diffusive flux in one dimension $j^2_{1,\xi}$ is

$$j^2_{1,\xi} = -D\frac{\partial C}{\partial \xi} - D'\frac{\partial \Pi}{\partial \xi} \tag{1}$$

The distance in polymer material coordinates, which corresponds to the volume per unit area of polymer, is $\xi = \int_0^x \rho_p \hat{V}_p dx$ with x the distance in lab coordinates, ρ_p the mass concentration of polymer, and $\hat{V}_p$ the partial specific volume of polymer (assumed to be constant). The concentration of solvent C is per unit volume polymer $C = \rho_s/(\rho_p \hat{V}_p)$, with ρ_s being the mass concentration of solvent. The quantity Π ([=] M/L^3) is proportional to the nonequilibrium contribution to diffusion potential; it represents a deviation of the total diffusion potential from the classical concentration potential for diffusion. Π is the *nonequilibrium contribution* to the diffusion potential, because it relaxes to zero with time at a constant concentration. Π turns out to be a memory integral of the local rate of polymer dilation $\sim \partial C/\partial t$ weighted by the (normalized) shear relaxation modulus φ_r in the mixture

$$\Pi = g(C)\left(\int_{-\infty}^{t} \varphi_r(C', t, t')\frac{\partial C'}{\partial t'}dt'\right) \tag{2}$$

Here $g(c) = G(C)/G_0$ with $G(C)$ being the instantaneous (high frequency) shear modulus and $G_0 = G(C = 0)$ being the shear modulus of pure polymer. D corresponds to the polymer material diffusion coefficient, related to D_{12}, the binary-mutual diffusion coefficient in physical coordinates, by $D = (\rho_p \hat{V}_p)^2 D_{12}$. The diffusion coefficient D' scales the flux down the gradient in the nonequilibrium contribution to the diffusion potential

$$D' = D\frac{\hat{V}_s^2 M_{ws} G_0}{RT}\frac{1}{(C\hat{V}_s + 1)}\frac{1}{(\partial f(C)/\partial C)} \tag{3}$$

$\hat{V}_s$ is the partial specific volume of the solvent, M_{ws} is the molecular weight of the solvent, R is the gas constant, T is temperature, $f(C) = \ln(a^*(C))$ is the local equilibrium fugacity of the solution, and $a^*(C)$ is the corresponding activity of the solution.

The diffusion flux $j^2_{1,\xi}$ from Eq. 1 is substituted into solvent continuity to give

$$\frac{\partial C}{\partial t} = \frac{\partial j^2_{1,\xi}}{\partial \xi} = \frac{\partial}{\partial \xi}\left(D\frac{\partial C}{\partial \xi}\right) + \frac{\partial}{\partial \xi}\left(D'\frac{\partial \Pi}{\partial \xi}\right) \tag{4}$$

This equation represents conservation of mass for 1-D mutual diffusion in a viscoelastic mixture. If the normalized shear relaxation modulus decays exponentially with a composition dependent relaxation time $\tau(C)$, $\varphi_r(C', t, t') = e^{-\int_t^{t'} dt'/\tau(C')}$, Eq.

2 can be differentiated with respect to time to give the differential equation

$$g(C)\frac{\partial C}{\partial t} = \frac{\partial \Pi}{\partial t} + \frac{\Pi}{\tau(C)} \tag{5}$$

This equation implies that the material relaxes with a single relaxation time while real materials exhibit a spectrum of relaxation times. Nevertheless this model should qualitatively reproduce the phenomena in real systems.

Equations 4 and 5 apply within the 1-D domain of the coating or film. For sorption, the film is in contact with a gas phase on both sides of the 1-D domain, and the solvent chemical potentials at the surfaces of the film are equal to the bulk phase gas value. For the drying of a supported coating, the diffusion flux in the mixture at the boundaries matches the external flux. This leads to the following boundary conditions for drying. At the substrate-coating boundary, the external flux is zero

$$j_{1,\xi}^2 = 0 \quad \text{at} \quad \xi = 0 \tag{6}$$

At the gas-coating boundary, the external solvent flux is proportional to the total drying force based on the solvent partial pressure drop between the coating surface and the bulk gas phase

$$j_{1,\xi}^2 = K_G P_s^* (a^+ - a^\infty) \quad \text{at} \quad \xi = l \tag{7}$$

K_G is a mass-transfer coefficient. The solvent partial pressure is the vapor pressure of pure solvent, P_s^* multiplied by the solvent activity a; the activities of solvent in the bulk gas and in the gas adjacent to the coating surface are a^∞ and a^+, respectively. The latter is presumed equal to the activity of solvent on the liquid side of the coating surface, a^-, which includes relaxation effects

$$a^+ = a^- = a^*(C)e^{[(\hat{V}_s M_{ws} G_0/RT)\Pi]} \tag{8}$$

Equations 6 to 8 and initial conditions of a uniform fluid concentration $C = C_0$, and zero nonequilibrium contribution to the potential $\Pi = 0$, provide the necessary auxiliary conditions to solve Eqs. 4 and 5 for isothermal drying.

Equations 5 to 8 include the physical properties of the solution (D, g, G_0, τ, a^*, $\hat{V}_s$, $\hat{V}_p$, M_{ws}, P_s^*) and the processing conditions (T, C_0, l, K_G, and a^∞). D, τ, g, and a^* are all generally concentration-dependent. Fu and Durning (1993) suggest that the normalized shear modulus g be assumed independent of concentration (i.e., $g(c) = 1$) as a reasonable simplification since the concentration dependencies of D, τ, and a^* are much more important in order to obtain qualitatively correct predictions. The equilibrium activity is approximated by $a^*(C) = C/C_{eq}$ where C_{eq} is the solvent concentration in solution at unit activity. Alternatively one can employ any of the standard solution theories, such as Flory-Huggins (Flory, 1953). In this article, the diffusion coefficient and the relaxation time are approximated as exponential functions of concentrations $D(C) = D_0 e^{kC}$ and $\tau(C) = \tau_0 e^{-mC}$ although more accurate descriptions (such as free volume expressions) (Vrentas and Duda, 1977) could be used. Using Eq. 3 and the foregoing approximations, the diffusion coefficient D' turns out to be

$$D'(C) = D_0' \frac{C}{(C\hat{V}_s + 1)} e^{[kC]}, \quad D_0' = \frac{D_0 \hat{V}_s^2 M_{ws} G_0 C_{eq}}{RT} \tag{9}$$

For numerical computation, Eqs. 5–8 were scaled using

$$z = \frac{\xi}{l}, \quad s = t\left(\frac{D_0 + D_0'}{l^2}\right), \quad u = \frac{C}{C_{eq}}, \quad \pi = \frac{\Pi}{C_{eq}} \tag{10}$$

which gives

$$\frac{\partial u}{\partial s} = (1-\alpha)\frac{\partial}{\partial z}\left(\bar{D}(u)\frac{\partial u}{\partial z}\right) + \alpha\frac{\partial}{\partial z}\left(\bar{D}(u)\frac{u}{\left(u\hat{V}_s C_{eq} + 1\right)}\frac{\partial \pi}{\partial z}\right) \tag{11}$$

$$\frac{\partial u}{\partial s} = \frac{\partial \pi}{\partial s} + \frac{\pi}{\theta \bar{\tau}(u)} \tag{12}$$

$$j_1^2 = 0, \quad z = 0 \tag{13}$$

$$j_1^2 = Bi(ue^{[(\alpha/1-\alpha)\pi]} - a^\infty), \quad z = 1 \tag{14}$$

$$u = \frac{C_0}{C_{eq}} \equiv 1, \quad \pi = 0, \quad 0 \le z \le 1 \quad \text{and} \quad s = 0 \tag{15}$$

In the above equations, $\bar{D}(u) = e^{[Ku]}$ and $\bar{\tau}(u) = e^{[-Mu]}$ represent the diffusion coefficient and the relaxation time in units of D_0 and τ_0, respectively. The parameters $M = mC_{eq}$ and $K = kC_{eq}$ measure the nonlinearity in the system; these lie between 5 and 20 for typical polymer solutions (Thomas and Windle, 1982; Fu and Durning, 1993). The set of dimensionless numbers set the relative importance of the main physical processes in the system

$$\alpha = \frac{D_0'}{D_0 + D_0'}, \quad \theta = \tau_0 \frac{D_0 + D_0'}{l^2}, \quad Bi = \frac{K_G P_s^* l}{C_{eq}(D_0 + D_0')} \tag{16}$$

α gives the fraction of the total flux due to elasticity effects. θ, a diffusion Deborah number (Vrentas and Duda, 1977) represents the relaxation time for the pure polymer τ_o, scaled with respect to the characteristic time for diffusion $l^2/(D_0 + D_0')$. The Biot number Bi represents the relative magnitude of internal to external resistances to solvent mass transfer.

The actual coating thickness h is a sum of polymer l and solvent l_s contributions. Both coating and solvent thicknesses can be calculated from the solvent concentration profile across the coating

$$h = \int_0^l (C\hat{V}_s + 1)d\xi, \quad l_s = \int_0^l C\hat{V}_s d\xi \tag{17}$$

The coating thickness can also be calculated from the initial value and the time integral of the solvent flux out of the coat-

ing, Eq. 7, multiplied by the solvent specific volume, $\hat{V}_s$. Both methods give the same value for coating thicknesses in our numerical solutions, demonstrating self-consistency.

Solution of Equations

Equations 11 and 12 are coupled, stiff nonlinear partial differential equations. They were solved by Galerkin's method with a trial solution comprised of piecewise continuous basis functions (cf., Strang and Fix, 1973; Finlayson, 1992). The coefficients of the time-dependent coefficients of the basis functions were found by solving the system of coupled differential-algebraic equations that express the requirement that the residual of each partial differential equation be orthogonal to the basis functions (Strang and Fix, 1973). The coated layer was divided into ten or more finite elements with u and π represented by quadratic polynomials across each element. Thus, the domain was spanned by a minimum of 21 basis functions, each associated with a node. The values of u and π were calculated as unknowns at each node.

For drying, the gradients in u and π were often steepest near the coating surface. Consequently, the elements near the surface were made smaller than those near the substrate by choosing $z_j \equiv ((j-1)/(nn-1))^2$, where z_j is the position of node j, and nn is the number of nodes (twice the number of elements plus one).

In the Galerkin formulation, the diffusive term of Eq. 11 is integrated by parts, and the boundary conditions, Eqs. 13 and 14, are applied to the resulting boundary terms. Three-point Gaussian integration evaluates the Galerkin residuals across each element (Strang and Fix, 1973).

We used a nonlinear differential-algebriac equation system solver, DASRT (a revised version of DASSL (Petzold, 1982; Brenan et al., 1989)) to solve the set of equations for the coefficients of the basis functions. DASRT used a variable order backward differentiation formula in a predictor-corrector integration scheme. The nonlinear algebraic system at each time was solved by a quasi-Newton method, where the matrix of sensitivities of the residual equations to the unknowns (Jacobian matrix) was only calculated when Newton's method did not converge within a specified number of iterations. The matrix of sensitivities of the residual equations was a square banded matrix (42 rows and columns for ten elements). Since the size of the matrix was relatively small, full Gaussian elimination was used for solving the linear system. This linear system was solved and the vector of unknowns was updated until the root-mean-square norm of the residuals converged to within 10^{-5} at each integration time step. DASRT automatically chooses the time integration step size and order of the backward differentiation formula to optimize speed of solution while maintaining the imposed error criteria. On a Cray Y-mp supercomputer, a typical run reported in this article took from between 4 and 10 CPU seconds for the complete integration.

Comparison with Published Results

The model presented here generalizes previous results to concentration-dependent physical properties and a nonzero external mass-transfer resistance. With proper specification of the parameters α, θ, Bi, M, K, u_o, and a^∞, the well established results for viscoelastic diffusion in sorption can be reproduced (Durning et al., 1985, 1986; Mehdizadeh and Durning, 1990; Fu and Durning, 1993). We show examples of two-stage sorption and Case II transport predicted by Eqs. 11 to 15.

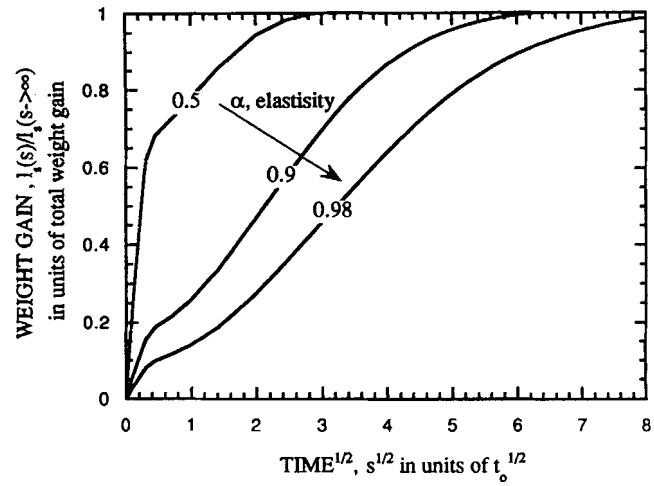

Figure 1. Prediction of relative weight gain in Two-Stage sorption into a thin film with parameters typical of the polystyrene-ethylbenzene for several values of α.

$\theta = 20$, $M = K = 5$, $u_o = 0.5$, $a^\infty = 0.51$, $Bi = 10^4$.

Two-stage sorption occurs during "differential" sorption into a thin polymer film where the activity of solvent in the gas changes by a very small amount. In this case, the concentration hardly changes and the diffusion coefficient and relaxation time are nearly constant. Predictions of weight gain using parameters typical for a thin polystyrene-ethylbenzene film (Billovits and Durning, 1990, 1993, 1994) are shown in Figure 1. Initially the solvent concentration rises rapidly near the free surface, causing a gradient resembling that during ordinary diffusion. At the same time, the weight gain increases rapidly. This rapid absorption (and consequent polymer deformation near the surface) causes a local rise in π. This causes a rise in activity at the surface of the film, and a consequent drop in the rate of sorption. For $\alpha = 0.9$, π rises to about 0.0015 near the surface of the film by $s = 0.1$; by Eq. 14 at this value of π and a concentration ~ 0.502 the driving force for sorption at the surface is near zero. Sorption into the film for times longer than $s = 0.1$ depends upon the relaxation rate of π. The weight gain at which the sorption rate suddenly drops depends upon α; higher α causes a faster rise in π at the surface and a smaller uptake before the drop in sorption rate. These predictions match well with those based on a linearized version of the model, and with experiment on the polystyrene-ethylbenzene system (Billovits and Durning, 1990, 1993, 1994).

Case II sorption occurs when the activity of solvent in the gas is increased a large amount from zero. Here, the concentration changes significantly during sorption, causing drastic changes in diffusivity and relaxation time during the process. A characteristic feature of Case II sorption is an induction time, in which the mass uptake is low, followed by an almost linear rate of sorption into the polymer material (Alfrey et al., 1966). The linear sorption rate corresponds to a sharp front in solvent concentration that propagates into the mate-

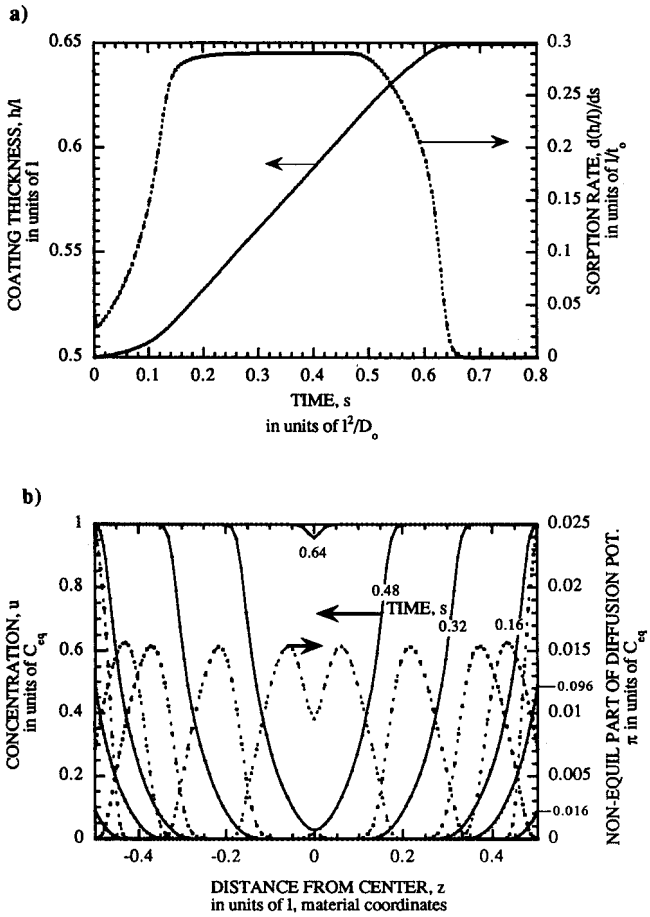

Figure 2. Prediction of Case II sorption with parameters typical of the poly(methyl methacrylate)-methanol system.

$\theta = 0.01$, $M = 5$, $K = 11$, $u_o = 0$, $a^\infty = 1$, $Bi = 5 \times 10^5$. a) Coating thickness and rate of change of thickness (dotted line) and b) u (solid lines) and π (dotted lines) profiles.

rial at constant speed (for Fickian, or viscous diffusion ($\theta = 0$), there is no induction time, and the rate of weight uptake decreases monotonically with time). These features are predicted in Figure 2 using parameters typical of poly(methyl methacrylate)–methanol near room temperature (Thomas and Windle, 1982), where Case II is readily observed. The weight uptake, proportional to the change in the film thickness h, starts low, but rises and becomes linear with time after the induction (Figure 2a). The constant rate of uptake is accompanied by a sharp front that propagates into the material at constant speed (Figure 2b). The cause of the sharp front is a peak in the nonequilibrium contribution to the diffusion potential π that retards fluid transport between the front and the surface but enhances it between the front and the film center. The result is a nearly uniform, relatively high concentration of fluid "held up" behind the front, with a nearly dry region of polymer on the other side. The peak in π travels just ahead of the concentration front at constant speed and retains a fixed same maximum value, about 0.015 in this case.

The results in Figure 2 are clearly characteristic of case II sorption and match results predicted from a simplified version of Eqs. 11 to 15 by Fu and Durning (1993), which corresponds to the original phenomenological model for case II proposed by Thomas and Windle (1982). In Figure 2, we used 30 finite elements to get smooth profiles of u and Π; the numerical solution did not change as we raised the number of elements above 30. That these calculations predict well-documented characteristics of sorption into viscoelastic materials validates the model and method of computation.

Predictions of Drying

The remainder of this article discusses predictions of isothermal drying from viscoelastic coatings based on Eqs. 11 to 15. This discussion is organized according to whether the diffusion is *viscous*, *viscoelastic*, or *elastic* (Vrentas and Duda, 1986). Viscous diffusion is ordinary, Fickian diffusion where the relaxation time is effectively zero ($\theta \ll 1$). Elastic diffusion corresponds to the opposite limit, where no relaxation occurs on the time scale of drying ($\theta \gg 1$). Viscoelastic diffusion is the intermediate case. In the viscoelastic case, we discuss the effects of α, M, K, and Bi on the drying kinetics.

Viscous diffusion ($\theta \ll 1$)

Figure 3 displays predictions of desorption from coatings where relaxation effects are absent ($\theta = 0$, $\alpha = 0$), and there is no external mass-transfer resistance ($Bi \gg 1$). In this case π is always zero, and the results correspond to Fickian diffusion. The coating thickness decreases monotonically and asymptotically approaches the dry coating thickness. The drying rate, equal to the time derivative of the coating thickness, decreases monotonically to zero from an initially large (negative) value (Figure 3b). With a high Biot number (i.e., a large mass-transfer coefficient), the solvent concentration drops to zero at the surface of the coating, while the solvent concentration gradient is steepest near the surface. The gradient decreases monotonically with time (Figure 3b). Because the diffusion coefficient increases with u through K ($\overline{D}(u) = e^{[Ku]}$), raising K results in faster desorption. Increasing the Biot number also results in faster desorption; although above $Bi = 100$, the change with Bi becomes negligible (cf., Cairncross et al., 1992).

Elastic diffusion ($\theta \gg 1$)

Equation 12 gives the relation between nonequilibrium contribution to diffusion potential π and the solvent concentration u. In a drying coating, the concentration at a material point nearly always decreases with time; so, π is normally negative during drying according to Eq. 12 and the initial condition $\pi = 0$. For large Deborah numbers ($\theta \gg 1$), the rate of change in π is roughly equal to that in u so that $\pi \sim u - u_o$ locally. Figure 4 shows this prediction with profiles of u and π for $\theta = 10^6$ and two values of α (0.5 and 0.98) with $M = K = 5$. Initially u and π are uniform at $u_o = 1$ and $\pi_o = 0$, and after a long time ($s \sim 1$ in Figures 4b and 4c) they are again uniform. For $\theta = 10^6$ and $\alpha = 0.5$ (Figure 4b), π does not have time to relax during drying, so that for $s > 1$, $u = 0$, and $\pi = -1$ persists indefinitely. At $\theta = 10^6$ and $\alpha = 0.98$ (Figure 4b), the time to remove solvent is much longer and π eventually begins to relax back to zero during the later stages of drying (above $s = 100$, $|\pi| < |u - u_o|$).

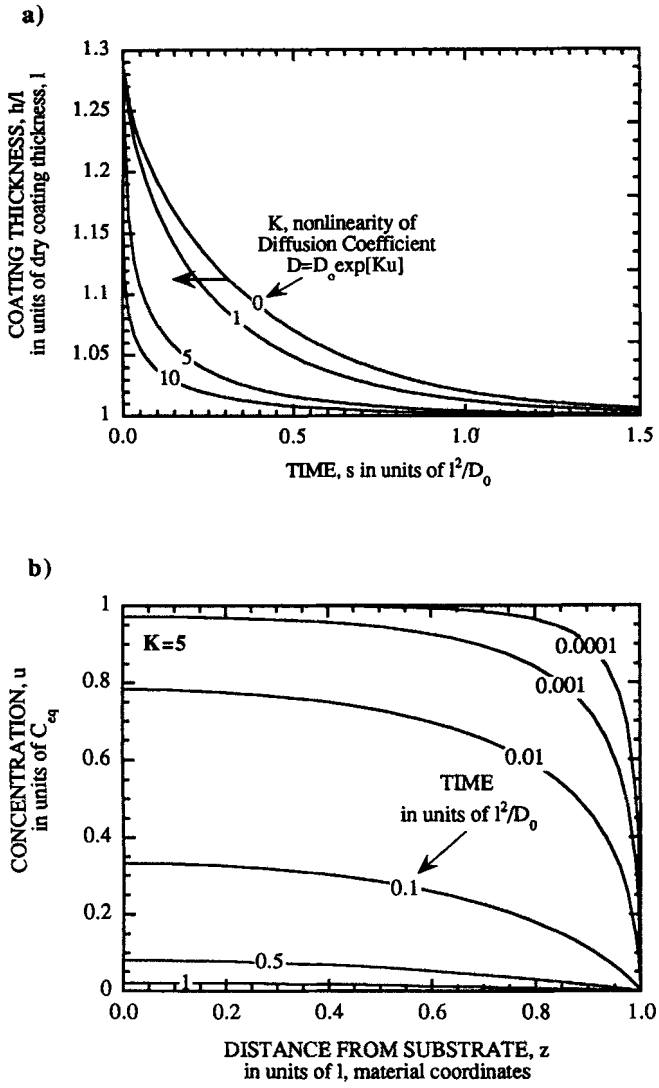

Figure 3. Viscous (Fickian) desorption from a coating without an external resistance.

$\theta = 0$, $u_o = 1$, $a^\infty = 0$, $Bi = 4.3 \times 10^8$. a) Coating thickness and drying rate (dotted line) for several values of K, the nonlinearity of diffusion coefficient, $D = D_0 \exp[Ku]$ and b) concentration profiles with $K = 5$.

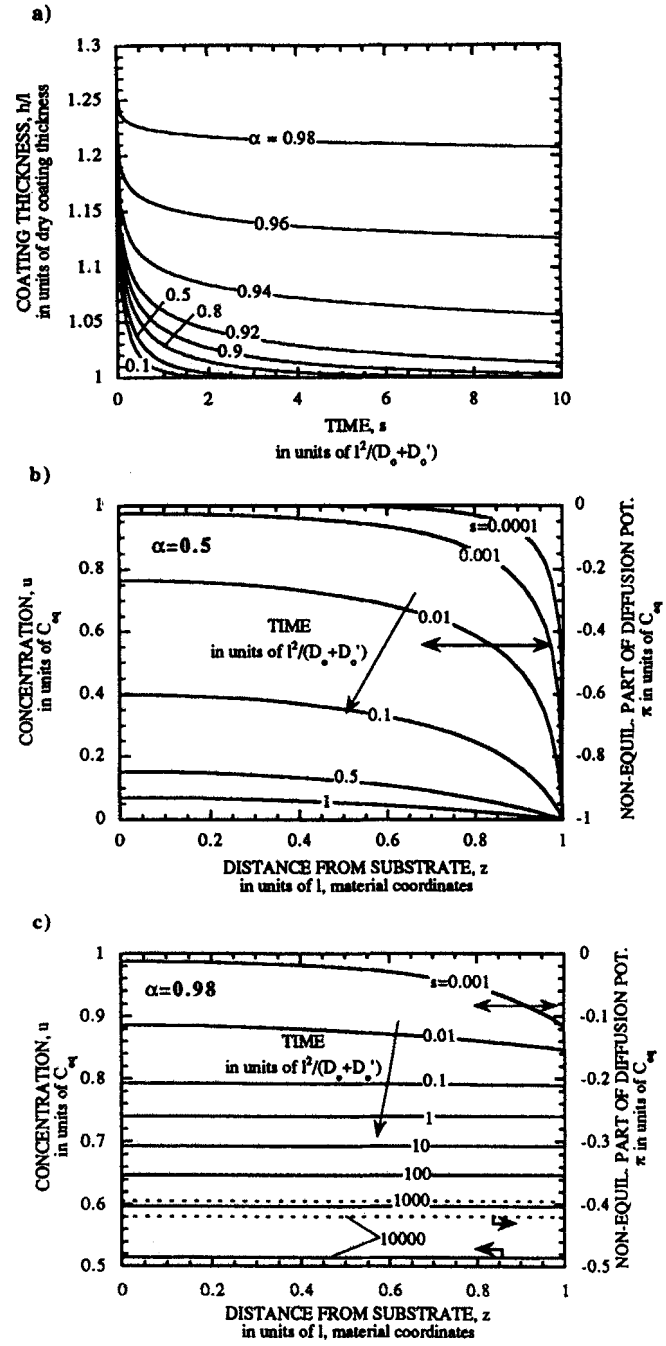

Figure 4. Elastic desorption from a coating.

$\theta = 10^6$, $M = K = 5$, $u_o = 1$, $a^\infty = 0$, $Bi = 10^4$ for various α. a) Coating thickness, b) u (solid lines) and π (dotted lines) for $\alpha = 0.5$, and c) u (solid lines) and π (dotted lines) for $\alpha = 0.98$.

Figures 4b and 4c show clearly that in the elastic limit, α plays a key role in the drying process. For $\theta \gg 1$, the rate of evaporation described by Eq. 14 falls as α increases, because at the surface of the coating, π is always negative and is near one. $[\alpha/(1-\alpha)]\pi$ becomes large and negative forcing $\exp[\alpha/(1-\alpha)\pi]$ to fall rapidly to zero. This cuts off the driving force for surface evaporation. Thus, the drying rate falls and the concentration at the free surface rises as α increases to near one in the elastic limit. In this case, the surface concentration can remain significantly above zero even at high values of the Biot number Bi, i.e., very little external mass-transfer resistance. Figure 4a shows that for $\alpha \sim 1$ the coating thickness plateaus at a value far above the dry coating thickness ($h = 1$). This final coating thickness is sensitive to α for $\alpha > 0.9$.

Figure 4c shows u and π for relatively high values of θ (10^6), α (0.98), and Bi (10^4). As described above, the change in π in this case follows that in u except at long times ($s > 100$). Despite the large value of Bi, which normally causes a precipitous drop in concentration near the free surface (Figure 3b), the concentration profiles are very flat, and the surface concentration remains significantly above zero. These concentration profiles resemble the result for externally controlled drying, at low Bi, primarily because $[\alpha/(1-\alpha)]\pi$ is negative and large enough that the effective resistance to evaporation becomes controlling. In this example, at $s = 0.1$,

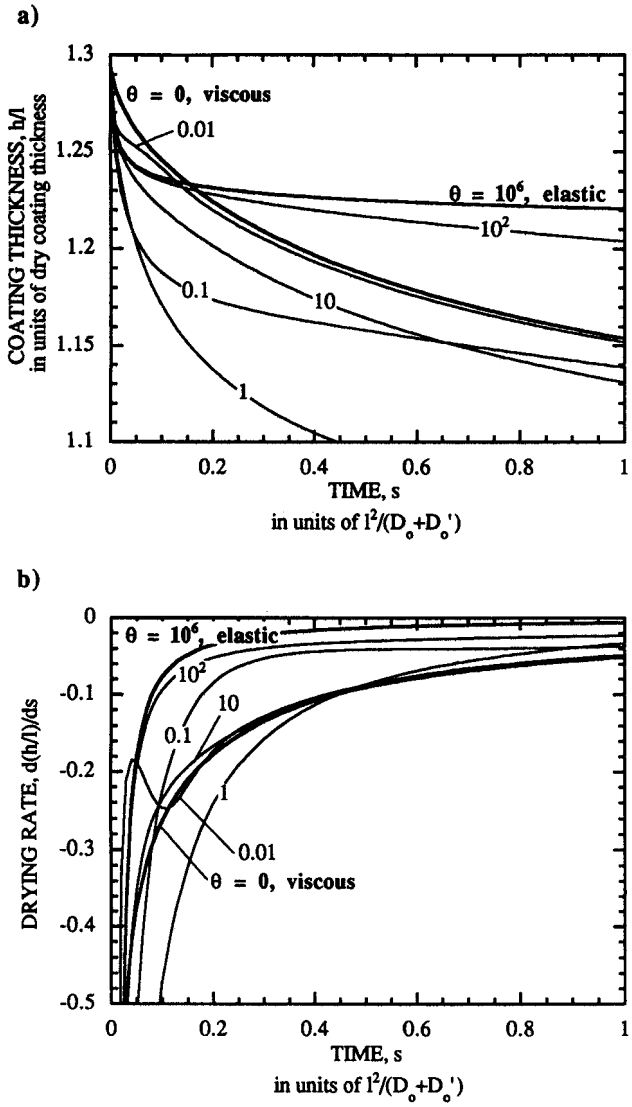

Figure 5. Viscoelastic desorption from a coating.

$\alpha = 0.98$, $M = K = 5$, $u_o = 1$, $a^\infty = 0$, $Bi = 10^4$ for various Deborah numbers, θ. a) Coating thickness and b) drying rate.

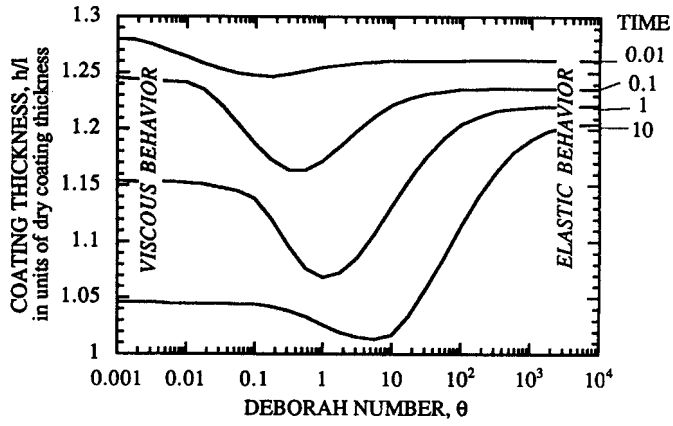

Figure 6. Effect of θ on coating thickness after a fixed drying time for viscoelastic desorption.

$\alpha = 0.98$, $M = K = 5$, $u_o = 1$, $a^\infty = 0$, $Bi = 10^4$.

$\pi \sim -0.21$, so the activity of solvent at the surface of the coating is reduced by $\sim 10^5$ from the value when $\pi = 0$. This reduction in surface activity nearly shuts off evaporation and causes the plateau in coating thickness shown in Figure 4a. Physically, α near one in the elastic limit corresponds to transport of a fluid in a very stiff elastic matrix which strongly resists collapse under the applied osmotic field.

Viscoelastic diffusion ($\theta \sim 1$)

At lower values of θ than in Figure 4, π relaxes locally during drying. The effect of θ on the coating thickness with time is shown in Figure 5 for relatively large values of α ($= 0.98$) and Bi ($= 10^4$) with $M = K = 5$. If the relaxation time is significant relative to the desorption time ($\theta > 0.1$) the rate of solvent removal is initially greater than for viscous diffusion ($\theta = 0$) because the gradient in π actually enhances diffusion during desorption (see below). However, if relaxation is not sufficiently fast ($\theta > 10$), then the external driving force for surface evaporation gets cut off and the coating thickness levels prematurely (as in the elastic case above), so that eventually the thickness predicted for viscous diffusion gets smaller than that for viscoelastic diffusion. Thus, an intermediate range of θ gives a minimum in the coating thickness after a specified drying time as shown in Figure 6.

Figure 6 shows the thickness of coatings in Figure 5 after specified drying periods ($s = 0.01$, 0.1, 1, and 10), as a function of Deborah number. At low and high Deborah number, the coating thickness reaches asymptotic limits corresponding to viscous ($\theta = 0$) and elastic ($\theta = \infty$) behavior respectively. For short times ($s \leq 0.1$), the viscous limit gives a thicker coating than the elastic limit, with a minimum in thickness at $\theta \sim 1$. At longer times ($s \geq 1$), the viscous limit gives a thinner coating than the elastic limit, the minimum in thickness shifts to a higher Deborah number ($\theta \sim 10$), and the minimum value gets closer to the viscous limit. From Figure 6, one sees that a small amount of viscoelasticity actually aids in solvent removal.

The minimum appearing in Figure 6 may correspond to trapping skinning in real systems (see the Introduction section). Lowering the Deborah number corresponds to increasing the initial coating thickness or lowering the product $\tau_0(D_0 + D_0')$ (see Eq. 16), which could be accomplished by raising temperature. Because Figure 6 shows that lowering θ can cause thicker coatings for fixed s in the low Deborah number portion of the plot, raising temperature can produce a thicker coating after a fixed real time.

Consider typical distributions of u and π in the viscoelastic regime (Figure 7) to clarify the competition between the elastic enhancement of diffusion in the coating and the effective increase in external resistance caused by nonequilibrium effects. Initially, the concentration drops faster near the free surface than in the bulk of the coating, so that the magnitude of π is large and negative immediately near the free surface. Thus, the nonequilibrium effect drives solvent toward the surface of the coating, enhancing the mass-transfer rate above the viscous (Fickian) contribution. This effect grows with θ in the viscoelastic regime. Figures 7a and 7b illustrate this with u and π for $\theta = 0.01$ and $\theta = 0.1$ corresponding to curves in Figure 5. Figure 7b shows that for $\theta = 0.1$, π has a steep negative gradient near the free surface that smoothes the

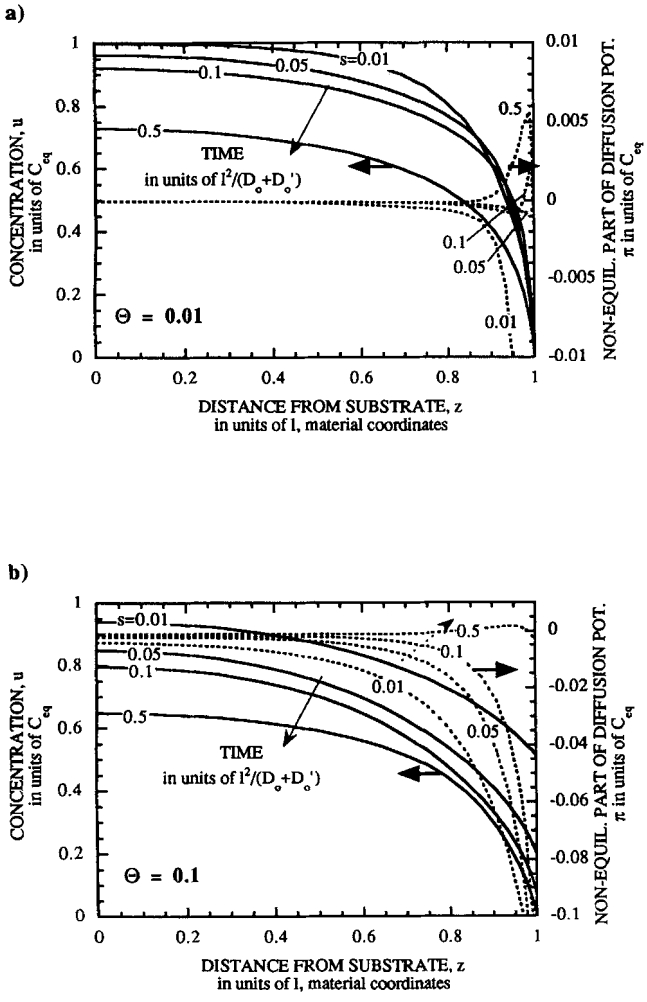

Figure 7. Viscoelastic desorption from a coating.

$\alpha = 0.98$, $M = K = 5$, $u_o = 1$, $a^\infty = 0$, $Bi = 10^4$. u (Solid lines) and π (dotted lines) profiles for a) $\theta = 0.01$ and b) $\theta = 0.1$.

gradient in concentration, and preserves a nonzero concentration at the free surface. In this case, the concentration contours resemble those for elastic diffusion (as in Figure 5a). At the lower Deborah number ($\theta = 0.01$ Figure 7a), diffusion due to the gradient in π initially smoothes the gradient in concentration, but because π relaxes to zero, a steep boundary layer in concentration does develop (Figure 7a). Here the concentration contours resemble those for elastic diffusion initially ($s < 0.05$), but those for viscous diffusion later ($s > 0.05$).

Thus, the minimum in coating thickness at intermediate Deborah number (as in Figure 6) arises from the enhanced internal diffusion due to a gradient in π but where π relaxes fast enough near the surface that the reduction in the evaporative external driving force (Eq. 14) is minimized. At Deborah numbers above the minimum in coating thickness, π does not relax fast enough near the surface, so that the effective external resistance becomes limiting. The appearance of a minimum in the coating thickness after a specified drying time in Figure 6 is the most important result of the calculations. In the remaining sections, we briefly summarize the effects of α, M, K, and Bi on the appearance of this minimum.

Effect of elasticity

The parameter α scales the relative magnitude of elasticity effects, which contribute to the driving force for diffusion. Lowering α from the value used in Figures 5 to 7 generally predicts faster drying as in the elastic limit (Figure 4), but it also decreases the difference between the thicknesses achieved at long times in the elastic limit ($\theta = \infty$) and in the viscous limit ($\theta = 0$). This makes sense when $\alpha = 0$, diffusion is purely viscous (Fickian) and independent of θ. Figures 8a and 8b illustrate this with predictions of coating thickness at specific times vs. θ for $\alpha = 0.95$ and $\alpha = 0.9$. At $\alpha = 0.9$, the minimum in coating thickness at intermediate θ is weak compared to that in Figure 6, and the coating thickness in the elastic limit is smaller than that in the viscous limit. At $\alpha = 0.95$, the minimum resembles that in Figure 6, although the coating thickness in the elastic limit is reduced. As in the elastic limit discussed in Figure 4, viscoelastic effects, including the minimum illustrated in Figure 6, are only evident for α in the range $0.9 < \alpha < 1$.

Effects of nonlinearity in diffusivity and relaxation time

The parameters M and K scale the change in relaxation time and diffusion coefficient with concentration. θ and α

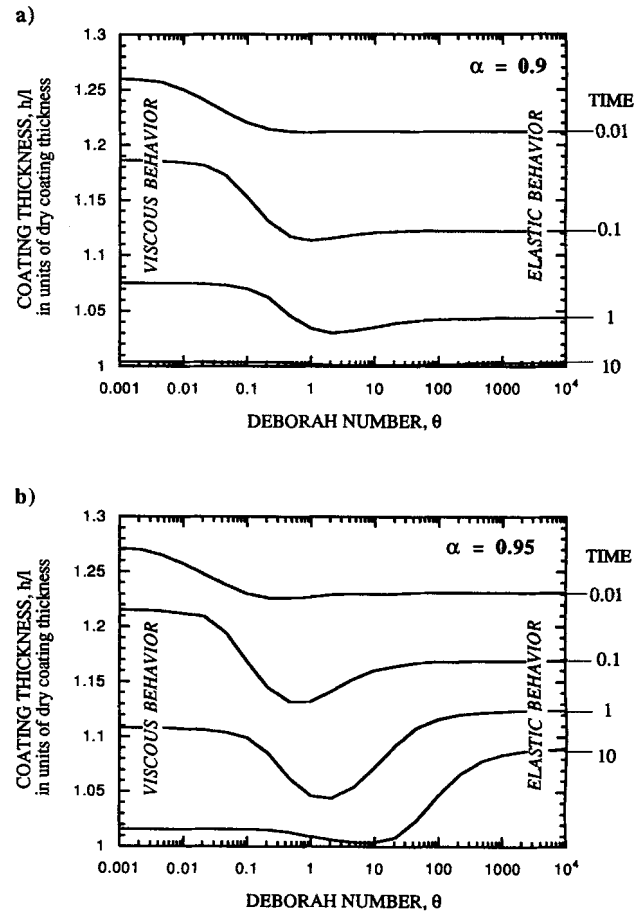

Figure 8. Effect of θ on coating thickness after a fixed drying time for viscoelastic desorption.

$M = K = 5$, $u_o = 1$, $a^\infty = 0$, $Bi = 10^4$. a) $\alpha = 0.9$ and b) $\alpha = 0.95$.

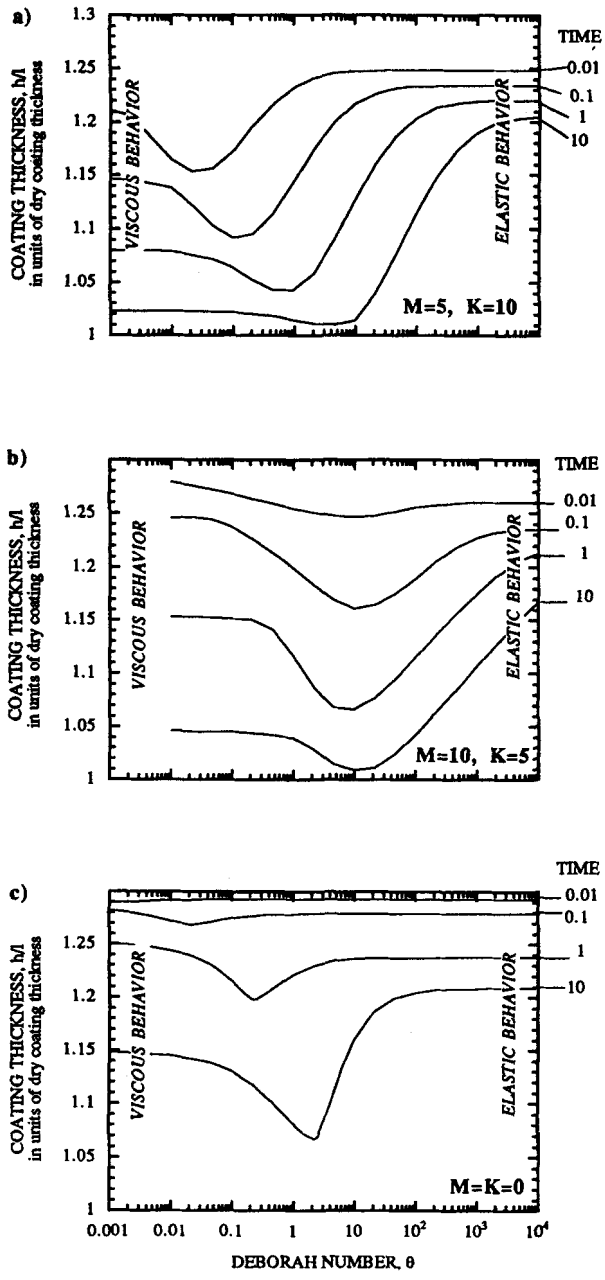

Figure 9. Effect of θ on coating thickness after a fixed drying time for viscoelastic desorption.

$\alpha = 0.98$, $u_o = 1$, $a^\infty = 0$, $Bi = 10^4$. a) $M = 5$ and $K = 10$ and b) $M = 10$ and $K = 5$, and c) $M = K = 0$.

are both defined in terms of the relaxation time and diffusion coefficient in the pure polymer ($C = 0$). If M and K are equal (as in all the previous results), then the product of the local relaxation time and diffusion coefficient, divided by the characteristic length squared, i.e., the instantaneous local Deborah number, remains constant. In Figure 9, the effect of unequal M and K is shown for $\alpha = 0.98$ for a range of θ.

For $K > M$ (Figure 9a), the local Deborah number increases with concentration. Consequently, the (spatial) average Deborah number during drying always lies below θ. So, the predictions of thickness after a fixed drying time vs. θ for short times when a lot of solvent is present in the coating get shifted to lower values of θ relative to the case $K = M$ (cf. Figures 9a and 6). Otherwise, the predictions are qualitatively similar.

When $K < M$ (Figure 9b), the opposite effect is predicted. Here the local Deborah number decays with concentration, so the average lies above θ at short times, when the solvent content is high. Consequently, the initial predictions in a thickness vs. θ plot are shifted to larger values of θ initially (cf. Figures 9b and 6). Note also that at higher M, the minimum in the coating thickness vs. θ becomes deeper.

Figure 9c shows predictions of coating thickness at specific times for a range of θ with both K and M set to zero; thus, the relaxation time and diffusion coefficient are constant at the dry coating values. We find generally slower desorption than the previous results, because the diffusion coefficient does not increase at higher solvent content. However, the minimum in coating thickness vs. Deborah number still exists near $\theta \approx 1$, although the minimum is sharper than in Figures 6, 9a, and 9b where the nonlinearities are included. Surprisingly, the nonlinearities associated with M and K do not have an important qualitative impact in desorption or drying, even though they completely change the character of the corresponding sorption process (such as Figures 1 and 2).

Effect of external mass-transfer coefficient

Cairncross et al. (1992) showed that the dimensionless time to dry a coating in Fickian (i.e., or viscous) diffusion decreases monotonically with rising Biot number. This result cannot explain observations of trapping skinning in polymer coatings. The model in this article also predicts a monotonic decrease in time to dry as Biot number increases (Figure 10). (If trapping skinning occurred in this model with respect to Bi, then the lines in Figure 10 would have a positive slope for some range of Bi). At both $\theta = 1$ and $\theta = 10^4$, the thickness after drying for a specified time falls with increasing mass-transfer coefficient. For the lower Deborah number, the coating thickness at $s = 10$ is insensitive to Biot number above $Bi = 100$. For the higher Deborah number, the coating thickness decreases logarithmically with Biot number for $s > 0.1$.

Discussion

According to the model discussed here, the rate of drying of viscoelastic liquid coatings is primarily determined by a balance of two factors: (1) Enhanced diffusion in the coating due to a gradient in π, the nonequilibrium contribution to the diffusion potential; and (2) reduced external driving force for surface evaporation due to the nonequilibrium contribution to the potential at the surface. These factors depend upon the physical properties of the solution and processing conditions. If the elasticity, expressed by α, and relaxation time θ are negligible, the nonequilibrium effects vanish and the Fickian model is recovered. Then the rate of drying rises monotonically with Bi and with K, which controls the increase of diffusion coefficient with concentration. If $\alpha \sim 1$ and θ is large ($\gg 1$), diffusion is "elastic." Then the nonequilibrium contribution to the diffusion potential does not relax during the drying process; the drying rate is initially rapid but the weight loss plateaus due to a "cutoff" of the effective external driving force. The effect of elasticity is only apparent

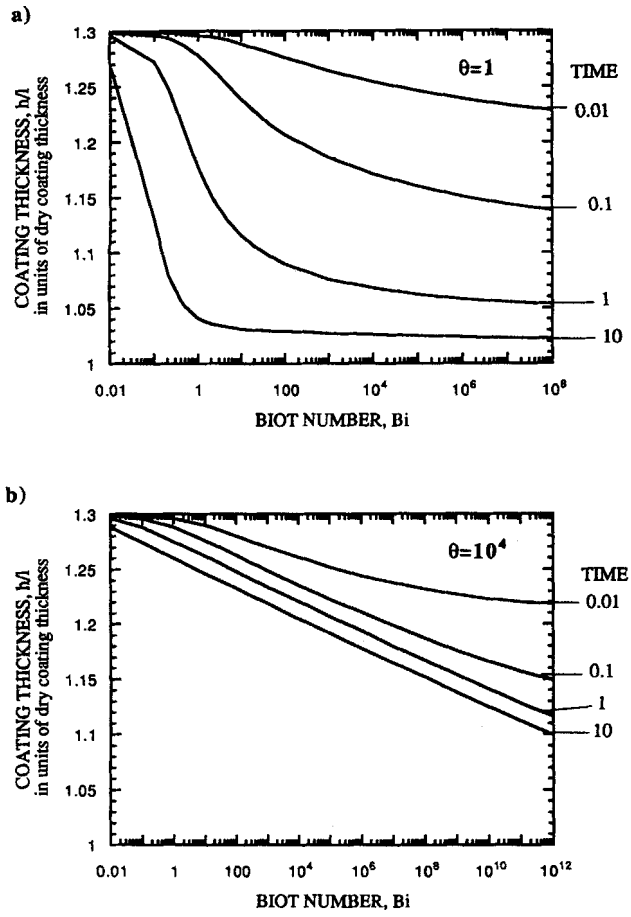

Figure 10. Effect of *Bi* on coating thickness after a fixed drying time for viscoelastic desorption.

$\alpha = 0.98$, $M = K = 5$, $u_o = 1$, $a^\infty = 0$. a) $\theta = 1$ and b) $\theta = 10^4$.

for $0.9 < \alpha \leq 1$; as α rises between 0.9 and 1, the coating thickness increases where desorption essentially shuts off.

For intermediate θ, where viscoelastic diffusion occurs, weight loss from a coating is initially faster than for viscous diffusion, because of the enhancement by π mentioned above, but the weight loss can plateau due to the reduced external driving force for surface evaporation. The latter effect is minimized if π can relax near the surface. Thus, viscoelasticity aids in solvent removal from coatings. As θ increases from the viscous to the elastic diffusion limit, the coating thickness after a specific time goes through a minimum, which occurs at $\theta \sim 1$. The depth of the minimum in coating thickness vs. Deborah number varies with the drying period s, the elasticity α, and the nonlinearity of diffusion coefficient K and relaxation time M. As the α decreases below 0.9, diffusion approaches the viscous limit and the minimum in coating thickness vs. θ disappears. As K increases, diffusion at short times is enhanced and the minimum in coating thickness vs. θ shifts towards smaller Deborah number. As M increases, the Deborah number corresponding to the elastic limit rises and the minimum in coating thickness rises to higher θ.

In all the situations considered in this article, the rate of desorption increases monotonically with mass-transfer coefficient *Bi*. If θ is large and π does not relax during drying, the coating thickness after a specified time decays logarithmically with *Bi*. For small θ, the coating thickness after a specified time reaches an asymptotic limit at high Biot number. Thus, the theory presented in this article does not provide direct predictions of the phenomenon of trapping skinning discussed in the introduction. Most reports suggest that trapping skinning results from increased airflow, i.e., increased *Bi*, but our results indicate that solvent removal always increases with increasing *Bi*. However, the minimum in coating thickness vs. Deborah number may correspond indirectly to trapping skinning because increasing temperature, which can reduce θ, is predicted to cause a thicker coating. Whether this type of trapping skinning occurs depends upon the sensitivities of diffusion coefficient and relaxation time with respect to temperature.

Acknowledgments

C. J. Durning acknowledges support from NSF (grant CTS 8919665) and the Coating Process Fundamentals Program at the Center for Interfacial Engineering (CIE) at the University of Minnesota. Helpful discussions with Regents' Professor L. E. Scriven at the University of Minnesota and Dr. P. E. Price at 3M are acknowledged.

Literature Cited

Alfrey, T., E. F. Gurnee, and W. G. Lloyd, "Diffusion in Glassy Polymers," *J. Poly. Sci.: Part C*, **12**, 249 (1966).

Anderson, J. E., and R. Ullman, "Mathematical Analysis of Factors Influencing the Skin Thickness of Asymmetric Reverse Osmosis Membranes," *J. Appl. Phys.*, **44**, 4303 (1973).

Beris, A. N., and B. J. Edwards, *Thermodynamics of Flowing Systems*, Oxford, New York (1994).

Billovits, G. F., and C. J. Durning, "Linear Viscoelastic Diffusion in the Polystyrene-Ethylbenzene System: Comparison Between Theory and Experiment," *Macromol.*, **27**, 7630 (1994).

Billovits, G. F., and C. J. Durning, "Linear Viscoelastic Diffusion in the Polystyrene-Ethylbenzene System: Differential Sorption Experiments," *Macromol.*, **26**, 6927 (1993).

Billovits, G. F., and C. J. Durning, "Two Stage Weight Gain in the Polystyrene-Ehtylbenzene System," *Poly. Commun.*, **31** 358 (1990).

Billovits, G. F., and C. J. Durning, "Polymer Material Coordinates for Mutual Diffusion in Polymer-Penetrant Systems," *Chem. Eng. Commun.*, **82**, 21 (1989).

Brenan, K. E., S. L. Campbell, and L. R. Petzold, *Numerical Solution of Initial-Value Problems in Differential-Algebraic Equations*, Elsevier, New York (1989).

Brown, W., and P. Stepanek, "Viscoelastic Relaxation in Semidilute and Concentrated Polymer Solutions," *Macromol.*, **26**, 6844 (1993).

Cairncross, R. A., L. F. Francis, and L. E. Scriven, "Predicting Drying in Coatings that React and Gel: Drying Regime Maps," *AIChE J.*, **42**, 55 (1996).

Cairncross, R. A., S. Jeyadev, R. F. Dunham, K. Evans, L. F. Francis, and L. E. Scriven, "Modeling and Design of an Industrial Dryer with Convective and Radiant Heating," *J. of Appl. Poly. Sci.*, **58**, 1279 (1995b).

Cairncross, R. A., et al., "Solidification Processes: a Critical Assessment," *Ind. Coatings Res.*, **3**, 1 (1995).

Cairncross, R. A., L. F. Francis, and L. E. Scriven, "Competing Drying and Reaction Mechanisms in the Formation of Sol-to-Gel Films, Fibers, and Spheres," *Drying Technol. J.*, **10**, 893 (1992).

Carbonell, R. G., and G. C. Sarti, "Coupled Deformation and Mass Transfer Processes in Solid Polymers," *I&EC Res.*, **29**, 1194 (1990).

Charlesworth, D. H., and W. R. Marshall, Jr., "Evaporation from Drops Containing Dissolved Solids," *AIChE J.*, **6**, 9 (1960).

Crank, J., *The Mathematics of Diffusion*, Oxford, Great Britain (1956).

Crank, J., and G. S. Park, "Diffusion in High Polymers: Some Anomalies and Their Significance," *Trans. of Farad. Soc.*, **47**, 1072 (1951).

Crank, J., "Diffusion in Media with Variable Properties," *Proc. Physical Soc.*, **63**, 484 (1950a).

Crank, J., "The Influence of Concentration-Dependent Diffusion on Rate of Evaporation," *Trans. of Farad. Soc.*, **46**, 450 (1950b).
Durning, C. J., and M. Tabor, "Mutual Diffusion in Concentrated Polymer Solutions under a Small Driving Force," *Macromol.*, **19**, 2220 (1986).
Durning, C. J., "Differential Sorption in Viscoelastic Fluids," *Poly. Sci. Poly. Phys. Ed.*, **23**, 1831 (1985).
Finlayson, B. A., *Numerical Methods for Problems with Moving Fronts*, Ravenna Park Publishing, Seattle, WA (1992).
Flory, P. J., *Principles of Polymer Chemistry*, Cornell Univ. Press, Ithaca, NY (1953).
Frisch, H. L., "Sorption and Transport in Glassy Polymers—A Review," *Poly. Eng. Sci.*, **20**, 2 (1980).
Fu, T. Z., and C. J. Durning, "Numerical Simulation of Case II Transport," *AIChE J.*, **39**, 1030 (1993).
Govindjee, S., and J. C. Simo, "Coupled Stress-Diffusion: Case II," *J. Mech. Phys. Solids*, **41**, 863 (1993).
Hui, C. Y., K. C. Wu, R. C. Lasky, and E. J. Kramer, "Case II Diffusion in Polymers II: Steady State Front Motion," *J. Appl. Phys.*, **61**, 5137 (1987).
Jou, D., J. Casas-Vazquez, and G. Lebon, *Extended Irreversible Thermodynamics*, Springer-Verlag, New York (1993).
Lasky, R. C., E. J. Kramer, and C. Y. Hui, "Temperature Dependence of Case II Diffusion," *Polymer*, **29**, 1131 (1988).
Lustig, S. R., personal communications (1994).
Lustig, S. R., J. M. Ceruthers, and N. A. Peppas, "Continuum Thermodynamics and Transport Theory for Polymer-Fluid Mixtures," *Chem. Eng. Sci.*, **47**, 3037 (1992).
Mehdizadeh, S., and C. J. Durning, "Prediction of Differential Sorption Kinetics near T_g for Benzene in Polysytrene," *AIChE J.*, **36**, 877 (1990).
Milner, S. T., "Hydrodynamics of Semi-Dilute Polymer Solutions," *Phys. Rev. Lett.*, **66**, 1477 (1991).
Neogi, P., "Anomalous Diffusion of Vapors through Solid Polymers: I. Irreversible Thermodynamics of Diffusion and Solution Processes," *AIChE J.*, **29**, 829 (1983).
Nicolai, T., W. Brown, S. Hvidt, and K. A. Heller, "Comparison of Relaxation Time Distributions Obtained from Dynamic Light Scattering and Dynamic Mechanical Measurements for High Molecular Weight Polystyrene in Entangled Solutions," *Macromol.*, **23**, 5088 (1990a).
Nicolai, T., W. Brown, R. M. Johnson, and P. Stapanek, "Dynamic Behavior of θ Solutions of Polystyrene Investigated by Dynamic Light Scattering," *Macromol.*, **23**, 1165 (1990b).
Petzold, L. R., "A Description of DASSL: A Differential/Algebraic System Solver," Sandia National Laboratories Report, SAND82-8637 (1982).
Powers, G. W., and J. R. Collier, "Experimental Modelling of Solvent-Casting Thin Polymer Films," *Poly. Eng. Sci.*, **30**, 118 (1990).
Shojaie, S. S., W. B. Krantz, and A. R. Greenberg, "Development and Validation of a Model for the Formation of Evaporatively Cast Polymeric Films," *J. of Mat. Proc. & Manuf. Sci.*, **1**, 181 (1992).
Strang, G., and G. J. Fix, *An Analysis of the Finite Element Method*, Prentice-Hall, Englewood Cliffs (1973).
Sun, Z., and C. H. Wang, "Light Scattering and Viscoelasticity of Polymer Solutions," *Macromol.*, **27**, 5667 (1993).
Thomas, N. L., and A. H. Windle, "A Theory of Case II Diffusion," *Polymer*, **23**, 529 (1982).
Thomas, N. L., and A. H. Windle, "Transport of Methanol in Poly(methylmethacrylate)," *Polymer*, **19**, 255 (1978).
Tsay, C. S., and A. J. McHugh, "Mass Transfer Modeling of Asymmetric Membrane Formation by Phase Inversion," *J. of Poly. Sci.: Part B Poly. Phys.*, **28**, 1327 (1990).
Vrentas, J. S., J. L. Duda, and W. J. Huang, "Regions of Fickian Diffusion in Polymer-Solvent Systems," *Macromol.*, **19**, 1718 (1986).
Vrentas, J. S., and J. L. Duda, "Diffusion in Polymer–Solvent Systems," *J. Poly. Sci.: Poly. Phys. Ed.*, **15**, 403 (1977).
Wang, C. H., and X. Q. Zhang, "Quasielastic Light Scattering and Viscoelasticity of Polystyrene on Diethyl Phthalate," *Macromol.*, **26**, 707 (1993).
Wang, C. H., "Dynamic Light Scattering and Viscoelasticity of a Binary Polymer Solution," *Macromol.*, **25**, 1524 (1992).
Wang, C. H., "Dynamic Light Scattering, Mutual Diffusion and Linear Viscoelasticity of Polymer Solutions," *J. Chem. Phys.*, **95**, 3788 (1991).

Manuscript received Feb. 6, 1995, and revision received Sept. 18, 1995.